



A discussion of a mechanism for isomerization of *n*-butane on sulfated zirconia

E. García^b, M.A. Volpe^a, M.L. Ferreira^{a,*}, E. Rueda^b

^a PLAPIQUI (UNS-CONICET), Camino La Carrindanga km 7, CC 717, 8000 Bahía Blanca, Argentina

^b UNS, Avda Alem 1253, 8000 Bahía Blanca, Argentina

Received 19 December 2002; received in revised form 19 December 2002; accepted 16 February 2003

Abstract

Although a huge amount of experimental work has been done, there is no clear picture about the superacidity in sulfated zirconia (SZ). Some authors think that sulfated zirconia is not superacid at all. Moreover, the structure of active site in *n*-butane isomerization is still now under controversy. This work tries to give some light about the mechanism of *n*-butane isomerization, taking into account experimental and theoretical works from others and from our own. MM2 and DFT simple calculations were performed in order to clarify the nature of the supported active species in sulfated zirconia. It is clear that a penta-coordinated species, monomeric or even dimeric, would be responsible for forming the most active sites at reaction conditions of *n*-butane isomerization. This idea is the key of this article. Different studies demonstrated that no superacidity is present before contact with *n*-butane. The sites formed at reaction conditions allow the *n*-butane dehydrogenation and its isomerization. A bimolecular mechanism of *n*-butane isomerization on penta-coordinated sites is proposed to occur. Several steps are discussed.

© 2003 Elsevier Science B.V. All rights reserved.

Keywords: *n*-Butane isomerization mechanism; Sulfated zirconia; Bisulfate species

1. Introduction

Despite the huge amount of experimental work done on sulfated zirconia (SZ), no clear picture about the structure of active species at SZ surface for alkane isomerization is presently available [1–3]. Moreover, there is growing evidence that superacidity might not be the source of the catalytic activity [3–9]. Redox and acidic–basic properties could be alternative sources of the activity of SZ in catalytic isomerization of hydrocarbons (specially *n*-butane). A variety of spectroscopic and surface sensitive techniques (infrared (IR),

NMR, XPS, HRTEM and others) were applied to study SZ. These studies were performed on SZ before the reaction, without alkane, or after the reaction. It is very difficult to study in situ the title reaction. In the open literature, theoretical studies involving a whole picture of the mechanism in *n*-butane isomerization are not found. The structures of the surface species in SZ involved in the intermediaries formation of the *n*-butane isomerization reaction has been not clarified until now [10–14]. When a H⁺ is presented no source is indicated. When a hydride is depicted, no sink is analyzed.

It was generally accepted until recent times that a stable tetragonal phase is necessary to obtain activity. Later, workers indicated that drastic sulfation to overcome the inertness of the surface makes catalysts out of the monoclinic oxide [15]. The route of drastic

* Corresponding author. Tel.: +54-291-4861700;

fax: +54-291-4861600.

E-mail address: mlferreira@plapiqui.edu.ar (M.L. Ferreira).

sulfation is not widely used. Sulfation is needed to improve acidic properties of ZrO_2 . Moreover, no considerable activity was found with ZrO_2 alone for *n*-butane isomerization. Two competitive mechanisms were generally proposed in the skeletal isomerization of *n*-butane, mono- or bimolecular in nature. The monomolecular mechanism involves the energetically unfavorable formation of a primary carbenium ion intermediate. In the bimolecular process, an octyl cation (C_8^+) is obtained by alkylation of the *sec*-butyl cation by butene before β -scission occurs. In case of the monomolecular mechanism, isobutane is the only product. With the bimolecular mechanism, sub-products (pentanes and propane) arise [16–19]. The time dependence for the reaction at low temperatures using SZ involves an induction period (where the only product is isobutane) and later a second period where subproducts evolve [20]. The induction period is shorter at high temperatures. Davis et al. [11] reported that in catalyst activity, the pre-treatment temperature after calcination procedure at 600°C is crucial. The results showed that an optimum in the conversion of *n*-butane was obtained when the catalyst was heated between 300 and 400°C prior to the reaction.

There are several points to take into account: source of sulfate group (H_2SO_4 or $(\text{NH}_4)_2\text{SO}_4$), the sulfation method, S final content, calcination procedure, pre-treatment temperature and the presence of H_2 . There is a lack of proposals of the steps and changes that must take place at the SZ surface to explain the observed experimental behavior in the open literature.

Being H_2SO_4 or $(\text{NH}_4)_2\text{SO}_4$ the S source, bisulfate is the main species present at the preparation aqueous media. We think that the supported S is present in different ways on SZ surface. Several active supported species have been proposed: dioxosulfate, monoxosulfate with tricoordination with surface and bisulfate group. These species can not explain some IR spectra and NMR data. Knözinger and coworkers [21,22] and White et al. [23] proposed monoxosulfate groups with multiple coordination sites with SZ surface as the main site. The presence of an OH bonding to S and to Zr in SZ is a very important issue. This site gives rise to Brönsted acidity. However, dimeric and polymeric species claimed to play a role [24]. Penta-coordinated S was proposed to be of paramount importance [23]. Lewis acidic–Lewis basic pair sites must be also considered in the analysis of the zirconia surface.

We performed a molecular mechanics and a simple DFT calculation on a model of sulfated zirconia. The aim was to clarify the structures of the SZ-most active species in *n*-butane isomerization. We propose a model that takes into account experimental and theoretical reported data. We also present experimental data of our own results using different routes of preparation of SZ with different S content. Although other workers have published results for the title reaction with similar catalysts, in this work we carried out a comparative study about catalytic activity from samples with a difference in the source of S and in the preparation methods. Moreover, this article is not an exhaustive theoretical or experimental study. This article presents a discussion of a possible mechanism with different aspects analyzed with different theoretical and experimental tools. The objective of this work is to present an alternative mechanism based on the in situ generation of the active sites for *n*-butane isomerization. Hydrogen effects, pyridine adsorption and experimental data are analyzed to correlate trends in its behavior. Some key aspects related to butene generation, *sec*-butyl cation formation, isomerization reaction at the proposed site and isobutane desorption reaction are studied with simple DFT. MM2 calculation on pyridine adsorption is also presented. The aim in this sense is to check qualitative trends in nature.

1.1. The methods

1.1.1. MM2

The used software was Chem 3D Ultra, version 5.0, 1999 (Cambridge Soft). Calculation using MM2 was performed on clusters of different sizes.

1.1.2. The surface models

The models considered for sulfated zirconia were monomeric and dimeric. The species I–IV are presented in Fig. 1(a). The dimeric species are claimed to be derivated from species IV, because water releasing, and they can be terminal or internal. Published FT–IR data [23,25] showed that no dioxosulfate groups are found at the prepared catalysts. From all these species, species IV and dimeric-terminal species from IV would show Brönsted acidity. From here, these species are IV-I and IV-II. Depending on the treatment temperature, the associated sites to site IV-I—the closest Zr site—from zirconia, changes:

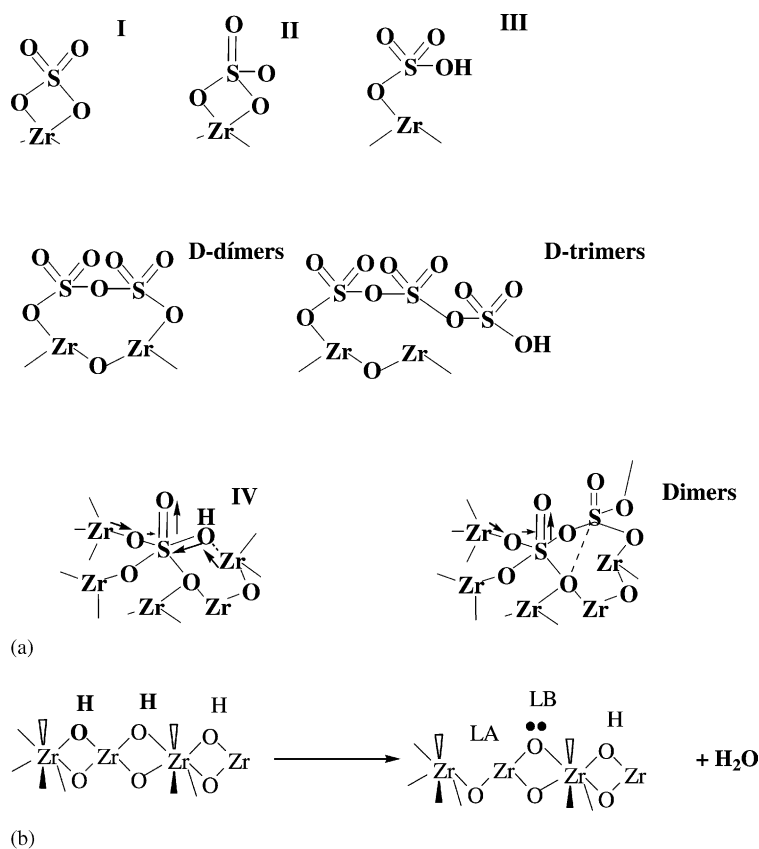


Fig. 1. (a) Proposed SO_4 species in SZ; (b) formation of LA–LB pair.

from Brønsted acid (BA) Zr-OH to Lewis acid (LB) Zr-O or Lewis acid Zr (LA) (see Fig. 1(a)). The presence of a LA site implies that a LB site was formed close to it. Since the calcination temperature generally used was 650°C [11] the associated site is considered to be a LA. This Zr (LA) is claimed to be highly reactive with water even at room temperature and a pre-activation procedure would be necessary to eliminate water before *n*-butane contacting. This LA has surely a LB site associated at zirconia surface, provided by dehydration process (Fig. 1(b)). Dissociative adsorption of water occurs over these LA–LB pair sites. Fig. 2(a) and (b) show the site IV formation in reaction conditions, involving *n*-butane and *n*-butene generation. Clearly, Brønsted sites arise from zirconia (Zr-OH-Zr) and from sulfated zirconia (S-OH-Zr).

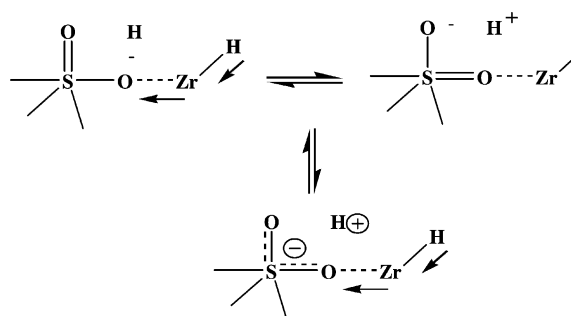
Higher pre-activation temperatures than 400°C in He flow decrease the Brønsted acidity from S-OH-Zr .

This Brønsted acidic site would almost disappear because of pretreatment at 600°C , and inactivation arises. Davis et al. [11] published that a very resistant Brønsted acidic site remains at surface up to this temperature. Temperatures higher than this destroy activity.

The two main exposed planes of tetragonal zirconia surface are (101) and (001) planes. They have Zr with coordination 6 or 7 to O, whereas O has coordination 2 or 3. Using MM2, a cluster of 8–10 Zr and a relaxed structure was considered. A structure with four Zr was also considered for comparison of dimeric and monomeric sites I and IV species.

1.1.3. DFT

The reaction of formation sites was investigated by means of DFT studies, using Gaussian'98 in a 512 Mb



(b)

Fig. 2. (Continued).

Several stages were considered in the calculation:

- The formation of the active site, with loss of water. In this stage, the stage of calcination or previous pretreatment to the reaction was simulated, since it is known that the water is a poison for these catalysts at high concentration on the surface [8].
- The formation of the *sec*-butyl carbocation.
- The isomerization to isobutane.
- The isobutane desorption.

Some alternatives related to the bifunctional site are also considered, presenting results with a model of disulfate species. The main point here is that the results are used in qualitative trends, not quantitative. With systems of few d electrons (involving Ti and Zr),

the bands energy in oxides is poorly represented by Gaussian. Moreover, the exact change in the surface electric field is very difficult to represent. So, there are few successful trials to study ZrO₂ using MM/QM coupled methods because of these problems. In this sense, the geometry of zirconia disposition at surface seems to be of huge importance.

2. Experimental

The catalysts of sulfated zirconia were prepared using the method of impregnation and immersion. The support, Zr(OH)₄, was obtained by precipitation of a aqueous solution of ZrOCl₂ with NH₄OH until pH 10 at ambient temperature. The obtained solid phase was washed with bidistilled H₂O until the complete elimination of chloride ions.

The sulfation of the samples was obtained by impregnation or immersion with (NH₄)₂SO₄ or H₂SO₄ at different initial concentration (see Table 1). The immersion method requires 15 ml of solution per g of catalyst during 45 min of contact. Other samples were obtained by immersion method with different volumes of H₂SO₄ 0.5N followed by drying on a hot-plate.

The samples were dried-off at 110 °C during 24 h and later calcined 4 h to 600 °C. They were characterized by XRD and content of SO₄²⁻ by LECO method. The BET areas of several of them were in the range from 90 up to 110 m²/g. Studies of pyridine

Table 1
Characterization of catalysts

Sample	Method	SO ₄ ²⁻ (g%)	FT-IR	XRD ^a (T%)	Conversion ^b (%)	
					Maximum	After 2 h
1	No sulfated	–	–	0	–	–
2	Immersion with (NH ₄) ₂ SO ₄ 6% nom.	4.6	L ≫ B pyridone	61	6.4	2.4
3	Impregnation with H ₂ SO ₄ 2N	3.0	L ≤ B pyridone ^c	38	4	1.7
4	Immersion with H ₂ SO ₄ 6% nom.	3.82	L ≤ B pyridone ^d	45	1.7	0.9
5	Immersion with H ₂ SO ₄ 20% nom.	12.8	L = B-vw pyridone ^e	100	7.0	4.3
6	Impregnation with (NH ₄) ₂ SO ₄ 6% nom.	4.11	L < B pyridone	39	0.9	0.4

^a Tetragonal:monoclinic ratio calculated as the peak height ratio between $2\theta = 30.1^\circ$ (tetragonal) and $2\theta = 28.7^\circ$ (monoclinic)—T% calculated from the peak height ratio.

^b Flow rate: 20 ml/min.

^c Well-defined bands.

^d Ill-defined bands.

^e Pyridone with the highest absorbance (vw: very weak).

adsorption were performed to evaluate the acidity of sulfated zirconia.

2.1. FT-IR studies of pyridine adsorption

Studies of adsorption of pyridine were done for all the tested samples. Using low amounts of solid, not more than 200 mg, a pretreatment of 2 h in N₂ (near 10 ml/min) at 150 °C was done. After this, the samples were contacted with flowing inert for 1 h at the same temperature in a pyridine reservoir. The samples remained 20 min in flowing N₂ to achieve the room temperature. At room temperature, we purged these samples by another 20 min. The data are included in Table 1. Using NaCl windows, we perform the FT-IR spectra in a Nicolet 520, with a resolution of 4 cm⁻¹ and 10 scans. We obtained signals of Lewis and Brønsted sites and pyridone complexes on these surfaces (at 1450, 1540 and 1635–1640 cm⁻¹). The spectrum of the bare windows was subtracted. Because of the known criticism to this method in the sense of over-consideration of LA sites [11], only the relative presence of each kind of site is included.

2.2. Reaction of *n*-butane isomerization

The catalytic test was carried out in a flow glass reactor operating at atmospheric pressure. The reactive mixture was 10% of butane in N₂. Approximately 100 mg of sample were pretreated in the reactor at 350 °C during 2 h under chromatographic airflow in order to activate the samples. Subsequently, the temperature was lowered to 200 or 100 °C and the reactive mixture was allowed to flow through the reactor at 20 cm³/min. The reactor was connected to a gas chromatograph (Shimadzu, GC-14B) provided with a TCD detector and a Chrom PAW 40/60 mesh column, working at 80 °C. The conversion of butane (*X*%), expressed as moles of butane converted percent, was taken as a measurement of the activity of the samples. The dependence of *X*%, at constant temperature and space velocity, on time, was measured. We have also calculated the selectivity to different products (*S*%). The selectivity to isobutane was calculated as:

$$S_I = \frac{\text{moles of isobutane}}{\text{total moles}} \times 100.$$

Table 2
Results for steric energy in a cluster of 8–10 Zr

Species	Steric energy (kcal/mol)
Non-terminal bisulfate	276.7
Terminal bisulfate	306.2
Sulfate at O bridge (reaction of 2OH)-1	313.9
Polysulfate (S ₃ O ₉ H)-BA	363.9
Sulfate by adsorption at LA-BA pair sites	428.7
Sulfate at O bridge (reaction of 2OH)-2	452.6
Sulfate at O of a Zr (both bridged)	462.4
Polysulfate (S ₃ O ₈)	560.3
Penta-coordinated S-Brønsted acid	267

3. Results and discussion

3.1. Methods

3.1.1. MM2

The results for steric energies are presented in Table 2 for different species tested at zirconia cluster of 8–10 Zr. A minor cluster was also tested to check penta versus tetrahedral coordination of S. The coordination of Zr was completed with OH. It is clear from Table 2 that penta-coordinated species like IV are the most probable in steric terms. We concluded that the most sterically probable species would be named IV, monomeric and dimeric. The other species have all problems: species I are not in agreement with IR studies. Species II presents a +5 oxidation state. Species III are claimed to be rather minor in concentration at surface. Polymeric species are considered to be at high concentration with S content higher than 2%. Species IV has S in +6 oxidation state and it takes into account several reported data about characterization. It is clear that Zr Lewis acidity is improved because of the withdrawing of electrons due to S=O presence in species IV (see Fig. 1). Brønsted acidity of site IV would be similar to zirconia in case of Zr-OH-Zr because the electronegativities of Zr and S are similar (2.3 versus 2.6). FT-IR data of pyridine adsorption showed that Brønsted acidity has almost no changes by sulfation, but Lewis acidity increases [2,28–30]. However, pyridine results must be considered with care. Davis et al. [31] found equal amounts of Lewis and Brønsted acid sites over sulfated zirconia after heating at 400 °C. Besides, the Brønsted-Lewis acids site ratio was essentially

zero after the sample was reactivated at 600 °C [31]. Previous studies showed that SZ was active for hydrocarbon conversions after activation at 650 °C [32]. These results are in agreement with the probability that the true catalytic sites are generated during the induction stage of the hydrocarbon conversion [33].

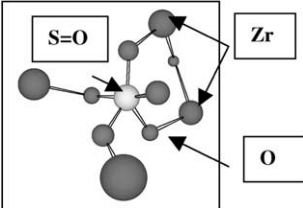
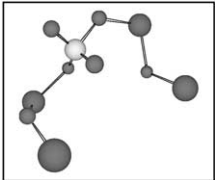
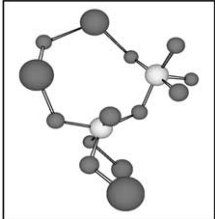
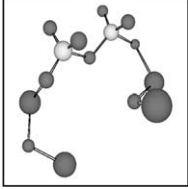

Several environments were considered, in agreement with the data presented above. The results of Table 2 can be explained taking into account the additional stabilization because of the SOHZr bond formation, resembling at surface tricoordination of O at bulk. The conversion of this site IV to II can occur by calcination at high temperatures because of water

evolution. A similar process is depicted in Fig. 1(b). The S in site IV is penta-coordinated, as in SOF₄, and S=O bond remains. The second S=O is proposed to react with a LA site of zirconia. The O⁻ of bisulfate reacts with a LA Zr. The remaining OH group reacts with a OH group of zirconia with water loss and generation of basic O. The fifth coordination of S is to a BA site of zirconia (see Table 3).

3.2. The mechanism

Any mechanism must explain the induction, the last period, the evolution of methane [34] and H₂ [13] at

Table 3
Results for steric energy (kcal/mol) in a cluster of four Zr no H depicted for clarity

Penta-coordinated S	302 (Zr 1 tetrahedral), 301.4 (Zr 1 trigonal plane)	
Dioxosulfate	523.8	
Dimer penta-coordinated S	334.9	
Dimer tetrahedral S	796.4	
		
		O Zr S

the initial stage. The mechanisms are proposed considering monolayer coverage of sulfated sites. Some of these sites are sites IV. This surface was selected taking into account the optimum ratio of LA:BA of near 2:1 found by FT–IR characterization of calcined SZ [35].

Sulfated zirconia acts as an isomerization catalyst at the induction period and as a cracking catalyst after that, in the absence of H₂ in the feed. This can be related to the hydride concentration at surface and the average lifetime of the carbonium ion. When it acts as an isomerization catalyst, hydride concentration is high and carbonium lifetime is short. As a cracking catalyst, hydride concentration is low and carbonium average lifetime is high [36].

3.2.1. The mechanism for the induction period

The mechanism for the induction period has sometimes reported to be monomolecular [19,20]. We propose that it could take place at monomeric sites IV-I and IV-II. Upon butane adsorption, partial reduction of one S⁶⁺ to S⁴⁺ takes place when sites IV-II are analyzed. The efficiency for reconversion to dimeric sulfate group is low. Deactivation arises because no regeneration of S–O–S bond in the case of sites IV-II. Conversion of *n*-butane shows a maximum with the time on the stream because the activation of the surface is necessary. Fresh species IV-II are active but they are present at low concentration, especially with low S content. The increase of temperature to 180–200 °C can avoid the low initial activity step at lower temperatures. In the induction period, the sites IV-I dehydrogenate *n*-butane at Zr(LA)–O(LB) pair sites, evolving H₂. Non-sulfated ZrO₂ is able to dissociate H₂ heterolytically [37]. H₂ can be dissociated by SZ, giving rise to H[–] associated to acidic Zr and H⁺ coordinated to basic O from ZrO₂. The site IV-I was developed taking into account the results of Lunsford et al. [38]. At this active site IV-I, H₂ evolution has two sources. One of them is direct dehydrogenation of *n*-butane in LA–LB pair sites (Hs' from different carbons). Another one is the carbonium ion (Hs' from the same carbon, penta-coordinated). Superacidity could be generated in reaction conditions, when butane is present (see Fig. 2(a)). An increased stability of the surface sulfate anion by charge delocalization could produce species with higher Brønsted acidity than the initial one, when no butane is present. This also occurs with

metanoate anion versus metanoic acid (see Fig. 2(b), highlighted species). The resulting anion by H⁺ loss would be a very weak base (see Fig. 2(a)). This species allows to the negative charge to follow the positive charge. The creation of a large potential energy for charge delocalization is avoided. This is especially true when C₈⁺ is considered [34,39]. Recent published work of Yamaguchi [40] based on isotopic analysis of alkane isomerization, pointed out that bimolecular mechanism is preferred on SZ for butane even at low temperatures, whereas it is not for *n*-pentane and *n*-hexane.

The dehydrogenation step leaves butene as an additional product, besides H₂. These butenes can be adsorbed on available acidic sites of zirconia. They can also react with available H. Sites with different Brønsted acidity and similar structure, strong and weak, to take place at SZ surface. On the strong sites, carbonium ions are formed upon butane adsorption. On the weak sites, desorption of isobutane leaves free the Zr(LA) site and the S–O–Zr bond without H (see Figs. 2(a) and 3). Butene reaction with C₄H₉⁺ adsorbed on S–O[–]–Zr leads to bimolecular mechanism. The carbenium–carbonium mechanism (C₄H₁₁⁺–C₄H₉⁺) takes place on S–OH–Zr. An alkoxy bond could be formed on Zr–O–Zr nearest to S–OH–Zr. The intermediary in isobutyl formation is methylcyclopropyl cation. Methyl group can react with hydride, generating methane. An allyl group remains coordinated by Zr(LA) close to S (see Fig. 4). Methane is not evolved from the protonated paraffin. Initially, at the induction step, no propane is found with isobutane (C₄H₁₁⁺ evolving CH₄ leaves C₃H₇⁺). Hong et al. [34] suggested that protonation by the strongest acid sites of sulfated zirconia is not the primary mode for initiation of butane isomerization. Basicity of O in SOZr bond is similar to O in Zr–O–Zr. Superacidity is lost because of hydride transfer to isobutyl cation and isobutane release. Regeneration or inactivation of S–OH–Zr is possible. Deactivation can be reversible because of H₂ dissociation reaction (see Fig. 4). Irreversible deactivation could take place, by reduction of sulfur (or even Zr) to lower oxidation states. Further dehydrogenation of adsorbed cationic species deactivates the site IV-I. H⁺ at surface can avoid this process. Only in the presence of a noble metal like Pt, the reactive H concentration is enough to hydrogenate these species

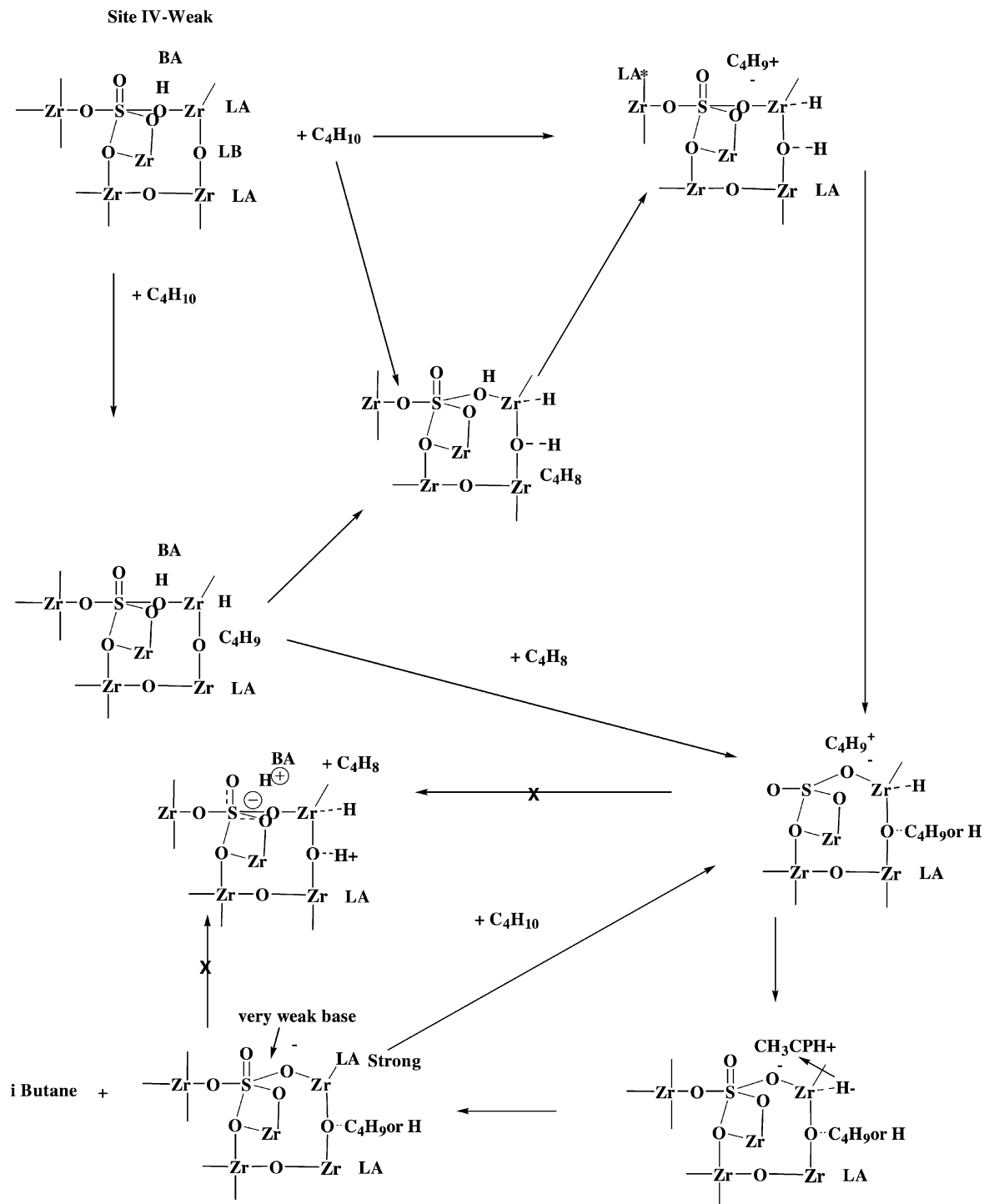
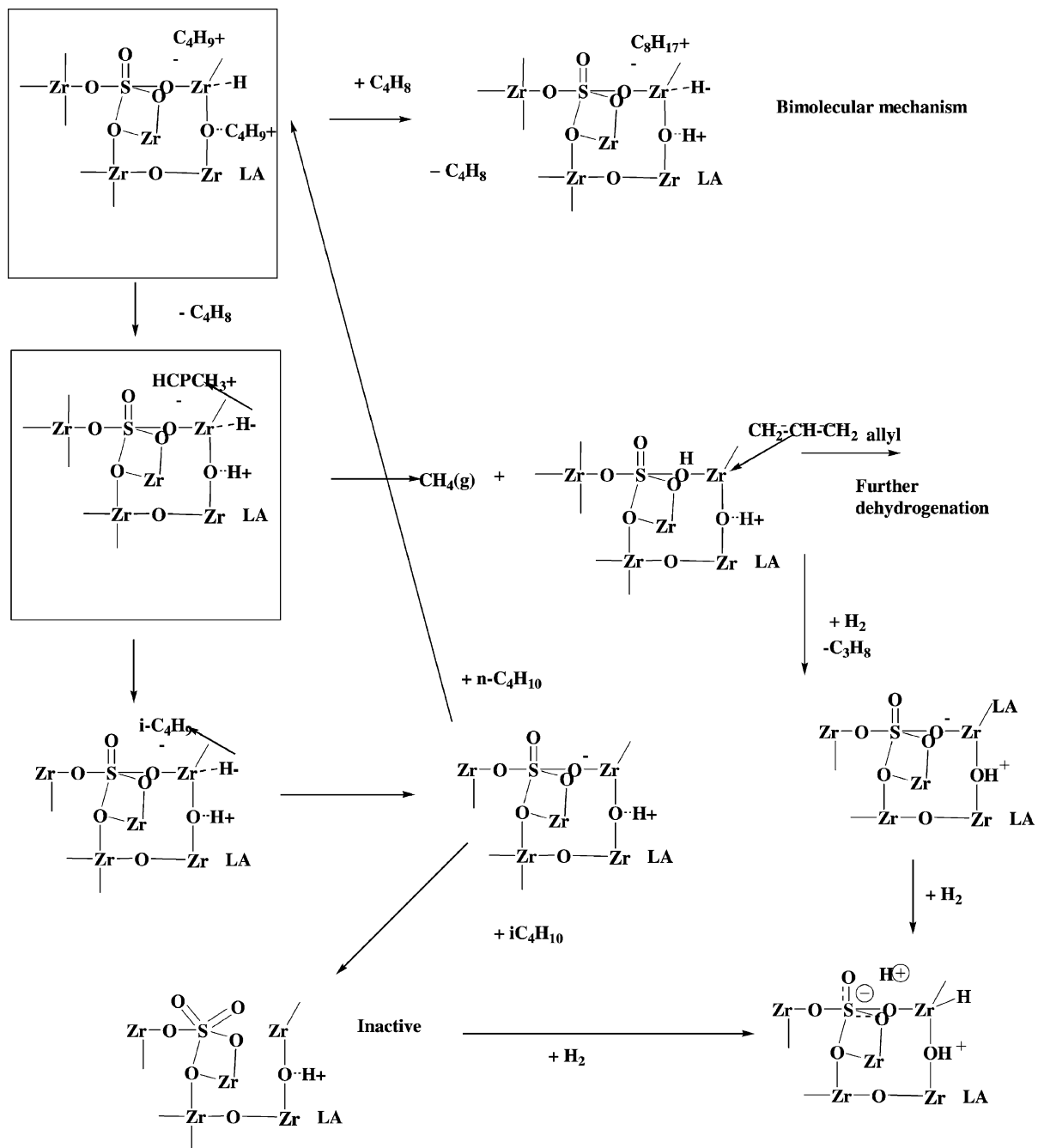


Fig. 3. Monomolecular mechanism for *n*-butane isomerization on "strong" acidic sites IV.

Fig. 4. Monomolecular mechanism for *n*-butane isomerization on "weak" acidic sites IV.

and avoid deactivation [31]. Hydrogen decreases the butenes concentration and, therefore, this effect is very dependent on its concentration.

Another termination reaction is the hydride abstraction from C_4H_{10} to carbonium ions. This reaction is energetically disfavored. No clear role of LA sites arises in this case. Gates et al. [36] published that catalytic activity for carbonium ion reaction is related to LA site concentration.

H_2 and n -butene formation would be possible on dimeric species—site IV-II (see Fig. 5). The weak point of this cycle is the regeneration of S–O–S bond. These sites could suffer irreversible deactivation although they could be the most active in monomolecular isomerization, but the most easily deactivated. $S^{4+}O_n$ forms a stronger base than $S^{6+}O_n$ because

$S^{6+}OH$ is a stronger acid than $S^{4+}OH$ in the case shown in Fig. 5. Therefore, H is placed on $S^{4+}O_n$ and inactive species are created.

In the monomolecular mechanism $C_4H_9^+$ has always a Zr–H close to it. Alcoxy groups adsorbed on Zr–O–Zr provide steric hindrance in its surrounding. It seems that the presence of Zr–H close to $C_4H_9^+$ is the main point. In bimolecular mechanism, never a $C_4H_9^+$ has a Zr–H close to it, because it reacts with the octyl-cation to evolve products (see Fig. 6). There is enough room for C_4H_8 coordination. A high coverage of the surface is needed and this is related to the n -butane pressure.

The induction mechanism can only be seen with the most active preparations, using low temperatures. Otherwise, at temperatures of 200 °C or higher, it takes

**MCP=methyl
cyclopropyl**

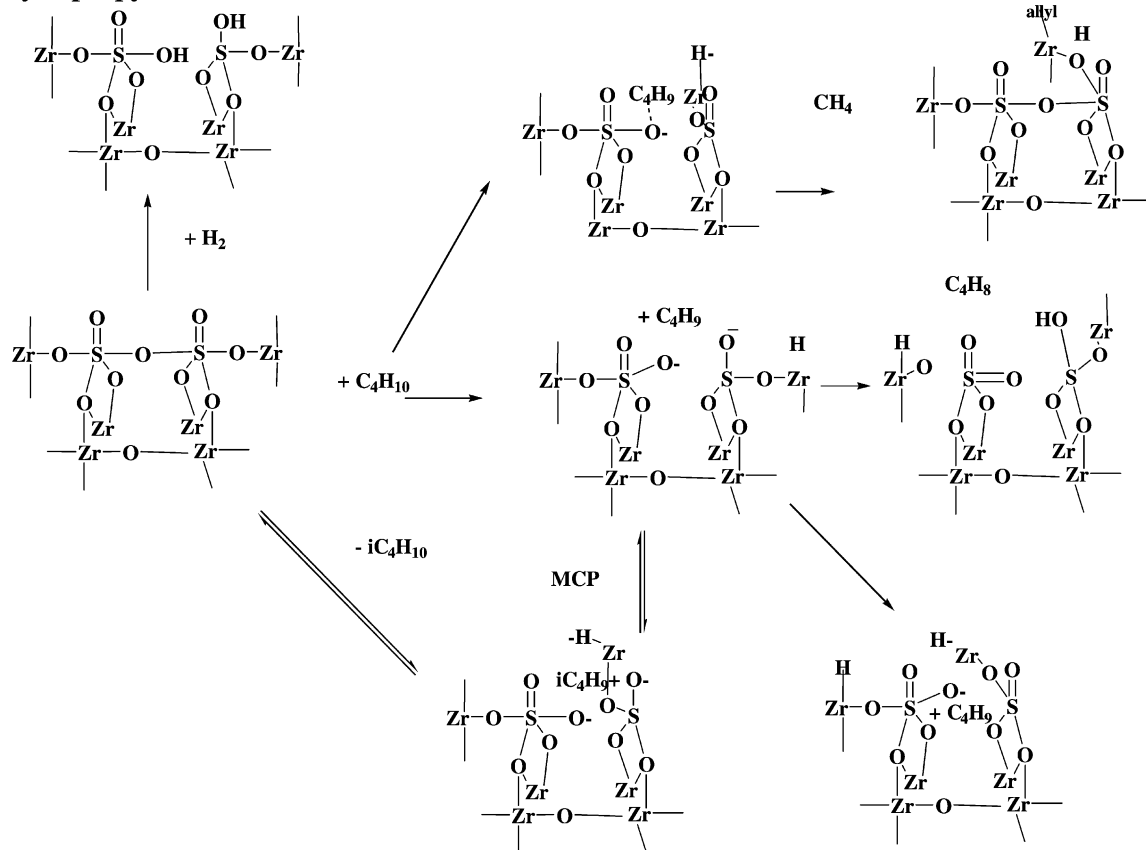


Fig. 5. Monomolecular mechanism for n -butane isomerization on dimeric sites IV.

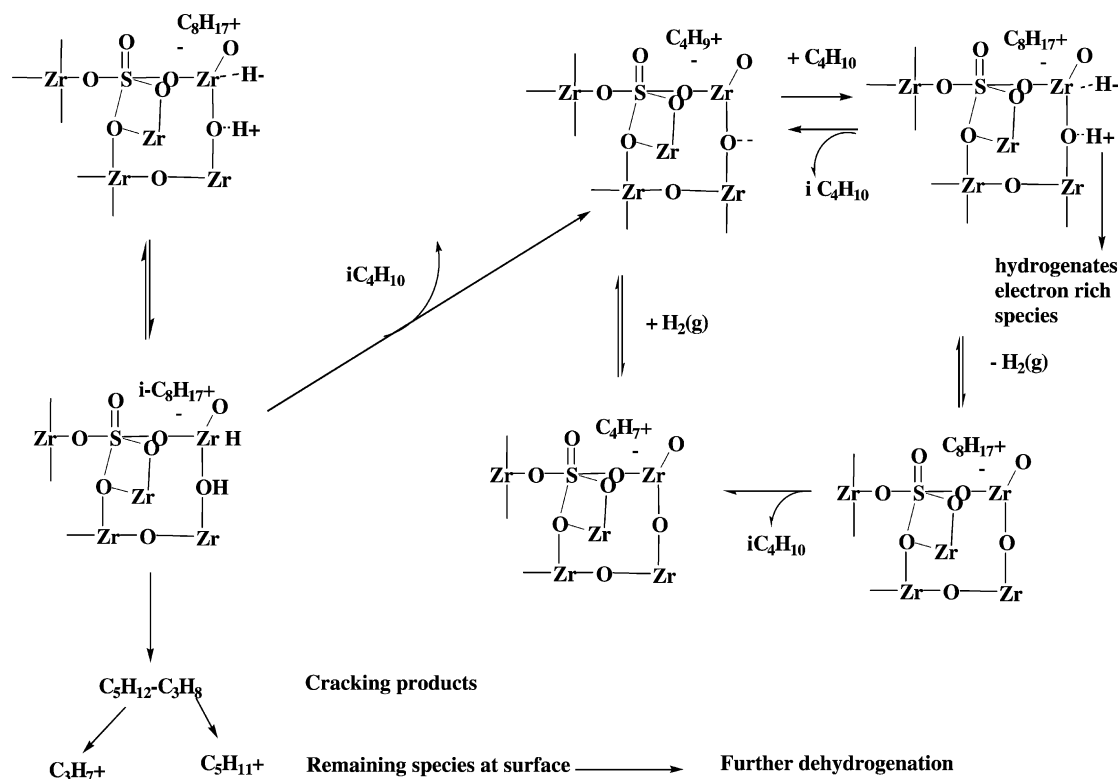


Fig. 6. Bimolecular mechanism for *n*-butane isomerization on "weak" acidic sites.

place at the first 1–2 min of the reaction. Quickly, the bimolecular mechanism begins to function.

3.2.2. Mechanism for the final period

This period presents evolution of by-products, mainly pentanes and propane. Therefore, a bimolecular mechanism is strongly supported by experimental evidence for *n*-butane isomerization. The bimolecular mechanism could take place on sites IV-I. In this case, *n*-butene concentration on the surface is high and the C_8^+ formation would be favored. The initial site IV-I has H⁻ (or a Zr-H bond) and H⁺ near the monomeric site (as OH). *sec*-Butyl cation is formed by reaction for site IV-I with butene. Addition of a second butene molecule produces the formation of octyl-cation. This is followed by the isomerization and β -C scission of C_8^+ . Reaction with another molecule of *n*-butane regenerates the active site SO-octyl-cation-Zr and Zr-H. Only one butene molecule triggers a chain reaction of *n*-butane isomerization. LB and LA sites

provide the necessary H⁺ and H⁻ to react with the isobutyl cation. Final release of isobutane is achieved. H⁺ from *n*-butane dehydrogenation can hydrogenate allylic species at surface, giving propane (see Fig. 5). Propane and pentanes are produced from C_8^+ cracking (see Fig. 6). Residual activity (activity at 2 h; see Table 4) could be assigned to sites resistant to reduction (polymeric). Besides, active sites after deactivation should be resistant to partial reduction of S and coke deposition.

The effect of butene (without H₂) is easy to understand: it triggers the *n*-butane conversion through a bimolecular mechanism. The increase of butene concentration produces the catalyst deactivation by allyl formation [41].

The switch from mono- to bi-molecular mechanism can be related to the structure of the active site proposed 2LA:1BA:1LB. If an alkoxy species is bonded to a LB site, hydride will be placed at Zr(LA) and a true ion-pair is formed. C_4H_9^+ is now a proton donor

Table 4
Activity and turnover rate (TOR) for catalysts presented in this and other works

Sample	Catalysts composition (sulfate content (%))	Temperature (°C)		Rate $\times 10^7$ mol/(g catalyst s)		TOR (s^{-1}) $\times 10^{3a}$		Carrier ^b (reference)
		Pretreatment	Reaction	Maximum	FP ^c	Maximum	FP	
2	(NH ₄) ₂ SO ₄ /ZrO ₂ (4.6)	350	200	9.5	3.3	1.99	0.69	N ₂ (this work)
3	H ₂ SO ₄ /ZrO ₂ (3)	350	200	7.2	2.7	2.30	0.87	N ₂ (this work)
4	H ₂ SO ₄ /ZrO ₂ (3.8)	350	200	2.5	1.7	0.63	0.42	N ₂ (this work)
5	H ₂ SO ₄ /ZrO ₂ (12.8)	350	200	10.7	5.8	0.80	0.44	N ₂ (this work)
6	(NH ₄) ₂ SO ₄ /ZrO ₂ (4.11)	350	200	1.3	0.6	0.31	0.15	N ₂ (this work)
–	(NH ₄) ₂ S ₂ O ₈ /ZrO ₂ (4.7)	450	250	–	2.2	–	0.45	Air [44]
–	H ₂ SO ₄ /ZrO ₂ 0.08N (5.75)	650	250	21.4	–	3.6	–	N ₂ [16]
–	H ₂ SO ₄ /ZrO ₂ (4.2)	500	50	4.8	–	1.1	–	N ₂ [12]
–	H ₂ SO ₄ /ZrO ₂ (3.33)	450	180	0.5	0.2	0.14	0.06	N ₂ [30]
–	H ₂ SO ₄ /ZrO ₂	–	–	2.5	–	–	–	He [43]
–	(NH ₄) ₂ SO ₄ /ZrO ₂ (2.9)	550	450	2.0	0.6	0.67	0.2	N ₂ [45]

^a The mol of butane converted to per mol of sulfate.

^b Recalculated values for our units and considering space velocity.

^c Final period, after 2 h reaction.

(acid) because of the anionic character of O. This reaction needs the coverage of the surface and activation of the alcoxy bond. It was found that dehydrogenation of butane takes place after an induction period [41]. The ZrO₂ is not active. Required acidity to trigger the reaction can be related to the LA site near the S–OH–Zr bond in sulfated zirconia. The LA sites of ZrO₂ are not enough acidic to abstract a hydride from *n*-butane.

The formation of *sec*-butyl cation (with Zr–H formation at the nearest Zr(LA)) was modeled on a cluster of eight Zr. The steric energy was near 183 kcal/mol, considering the formation of a carbocation and a negative O at surface. The bimolecular mechanism was checked with the same site, by reaction with a butene molecule. The C₈⁺ formation implies 190.1 kcal/mol. A difference of only 7.1 kcal/mol in steric energy with the monomolecular mechanism was found.

3.2.3. DFT

Recent data were published about DFT studies on SZ. Kanougi et al. [27] presented calculation on structural properties as well as electronic states of the surface. This article was focused on H₂SO₄ reaction with zirconia surface to afford water and SO₃ in agreement with Haase and Sauer [5]. These authors did not take into account the experimental step of calcination, where water is lost and subsequent reordering must be considered. In this sense, refs. [5,27] present only pre-

cursors of the active sites. Another point to consider is the relaxation of surface at this level.

Only 10% of the active sites in SZ are the most active [34,42]. In this sense, active site is a minor structure. With this idea in mind, we included an active site with SOHZr bond. Clearfield et al. [10] suggested that some bisulfate structure is stable until 600 °C.

Fig. 7 presents the results for the IV and I sites formation. The value for dioxosulfate formation is similar to that reported by Kanougi et al. [27], –55.4 versus –59.2 kcal/mol. In the theoretical studies of this kind, it is important to consider that H₂SO₄ and HSO₄[–] concentrations change with solution concentration, pH, sulfate agent used (H₂SO₄ or (NH₄)SO₄) and the presence of water in the neighborhood. Water is lost at the calcination step and surface rearrangement arises. In fact, no water is lost from site IV because of geometric considerations. From site I, water is weakly adsorbed and easily released. Taking into account these points, we included a DFT study using Gaussian'98W in a small model of the structure, resembling the claimed penta-coordinated S (see Fig. 8(a) and (b)). We did not include the C₈⁺ formation in this work because the preliminary results indicate that our simple model can not afford the complete interaction of the C₈⁺ with the sulfated zirconia surface. Several sites are involved in the C₈⁺ stabilization at surface. The main results of the calculation were: endothermic character of butene formation at first (+77.8 kcal/mol), exothermic reaction

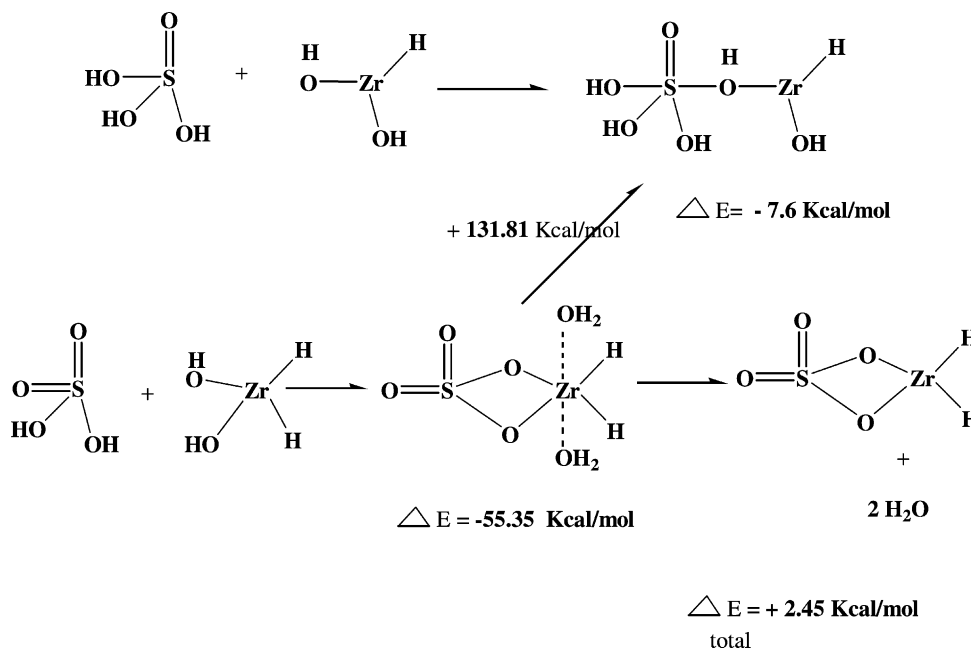


Fig. 7. DFT results for sites I and IV formation.

for *sec*-butyl formation (−28.1 kcal/mol), endothermic isomerization to *tert*-butyl cation (32.4 kcal/mol) and finally exothermic character for isobutane desorption (−86.9 kcal/mol; see Fig. 8(b)). The initial structure is not regenerated. The leaving site is an extremely weak base. Zr is a strong Lewis acid and can extract hydrogen from butane. The *sec*-butyl cation formation from this site is endothermic in 54.5 kcal/mol.

A simple calculation of *sec*-butyl cation formation on sites IV-II suggested that this reaction is possible and endothermic by 115 kcal/mol (with parallel reduction of one S^{6+} to S^{4+}). Isomerization to *tert*-butyl cation is possible, with a change in energy of −1.2 kcal/mol. The cycle involved in the regeneration of these sites is the weaker aspect of the mechanism, because S^{4+} should be re-oxidized.

3.2.4. The *n*-butane isomerization

Tables 1 and 4 show the catalyst characterization and *n*-butane reaction results, respectively. Selectivity to isobutane is always near 95%. Reactions at 100 °C gave very low activity and results are not shown. It is clear from Table 1 that the immersion method is better than impregnation for $(NH_4)_2SO_4$. The main difference between procedures is the presence of the tetrag-

onal phase in higher amount (61 versus 39%). Also, the amount of Lewis acidic sites in case of immersion procedure is higher. In case of using H_2SO_4 (Samples 3 and 4) the structure in terms of FT-IR and XRD is similar. The tetragonal phase is present at higher concentration in Sample 4. Initial conversion is clearly different. This result is in line with those published by Stichert et al. [45], where the authors proposed that not only the acidity of sulfated zirconia determines the catalytic performance, the surface structure is also important. The bimolecular mechanism needs a favorable arrangement of surface groups. Tetragonal system or drastically sulfated monoclinic structure in SZ is especially suitable for this.

The presence of dimeric or polymeric sulfate species-sites IV-II, with lower activity, could decrease the turnover rate (TOR; see Table 4). Immersion procedure using high amounts of sulfate increases the conversion to isobutane. The TOR in these conditions is lower than the TOR of samples with lower amounts of sulfate (comparing Table 4, Samples 3 and 5). The TOR in Sample 4 is lower than Samples 2 and 3. In Sample 4, the only crystalline phase is tetragonal. The Samples 2 and 5 have the maximum rate while Samples 4 and 6 the lowest. The TOR follows the trend

found for maximum TOR. From comparison of our results with those reported in the literature, we observed that persulfate as precursor does not improve activity at 2 h reaction.

3.2.5. FT-IR data for pyridine adsorption

SZ presents the bands of adsorbed pyridine at 1540 (BA), 1445 (LA) and another band at 1640 cm^{-1} . These bands arise when SZ is heated at 650°C and evacuated at $400\text{--}600^\circ\text{C}$. Band at 1640 cm^{-1} is as-

signed to pyridone [21]. The pyridone band is not present in bare ZrO_2 . The site IV-I gives rise to this band because of steric hindrance for pyridinium formation [11]. The other bands can be assigned to LA sites with different environments (see Fig. 9(a)). On the other hand, Morterra and Cerrato [46] showed that, in the case of SZ the use of pyridine adsorption as a titration method to obtain Lewis/Brønsted (L/B) acidic sites ratio could lead to unreliable results [47]. In our cases, we think that the Lewis acidic sites and pyridone

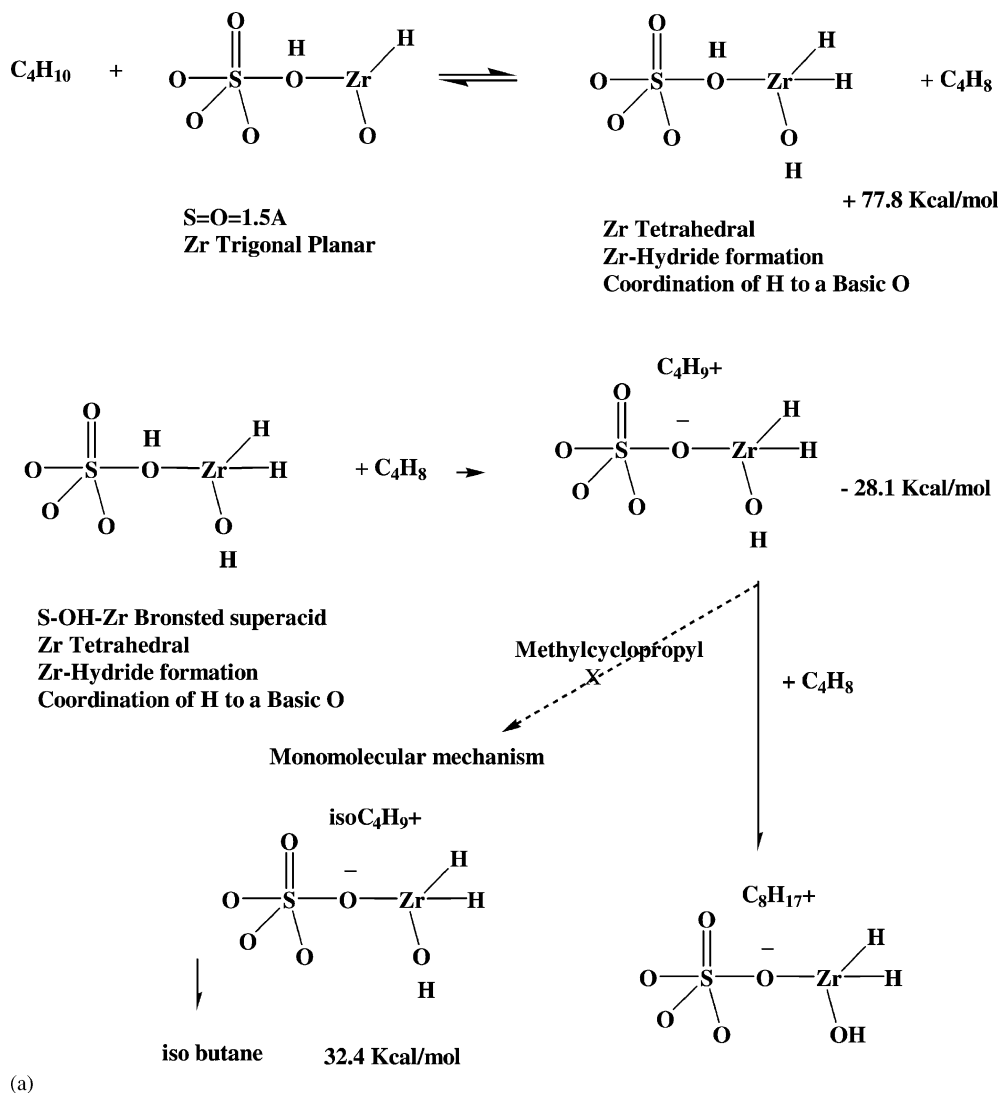


Fig. 8. (a) DFT results for coordination of butene and isomerization to *tert*-butyl cation; (b) DFT results for desorption of isobutane and coordination of a new butane.

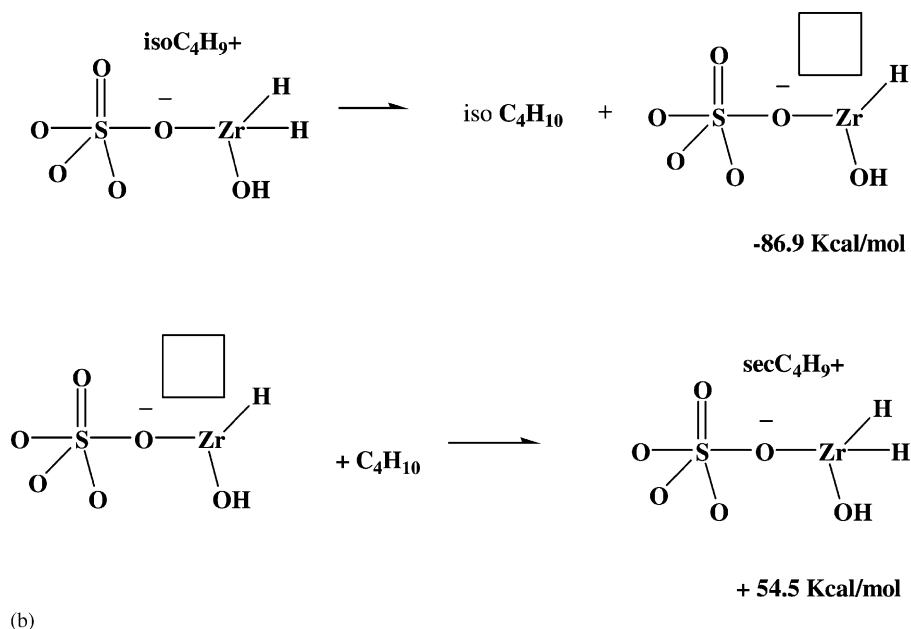


Fig. 8. (Continued).

presence before reaction are important data to correlate with the activity of the sample. The existence of sterically hindered hydrogen bonded to a S–O–Zr bond is crucial. The best catalyst is found when Lewis acid sites and pyridone are present together (see Table 1) [48–50].

Fig. 9(b) and (c) show the calculation results using MM2 for pyridine adsorption on LA (35 kcal/mol) on BA (152 kcal/mol) and on LA–BA pair (92 kcal/mol). Lewis acid sites and LA–BA pairs are the preferred sites for adsorption of pyridine when no butane is present. Remember that the Brønsted acid in SZ at this stage is not superacidic. It has almost the same acidity as Brønsted acid in ZrO₂. The Lewis acid site (Zr) is stronger than the Brønsted one (S–OH–Zr) in the site IV-I. A competition between both takes place for pyridine adsorption. The pyridine is adsorbed first on the LA site. After adsorption on the Lewis site, when pyridone is found the C–O bond is formed from reaction of C-2 of pyridine with OH from S–OH–Zr.

3.2.6. Lewis and Brønsted acid sites

Published data stressed the importance of the activation temperature before the reaction [20,51,52]. Arata [51] and Matsushashi et al. [20] reported that isomeriza-

tion proceeds by monomolecular mechanism on Lewis acid sites. On the other hand, surface alkenes have claimed to be produced on the Brønsted acid sites. We do not agree with this idea. Monomolecular mechanism needs LA and BA sites. Bimolecular mechanism needs BA sites [53].

3.2.7. Effect of carrier-effect of H₂

It is clear that adding H₂ assures enough H[−] and H⁺ concentration at surface, because of heterolytic cleavage at LA–LB sites (strong, near monomeric active sites, weaker, at zirconia LA–LB pairs). The H₂ at the monomeric site cycle avoids allyl species accumulation. It can also regenerate in situ superacidity. At the dimeric site, it increases the concentration of protonated species. The possibility of reaction of surface H with migrating *n*-butenes at surface is higher in the presence than in the absence of H₂. All the dehydrogenation reactions are disfavored (see H₂ effect in Figs. 3–7). However, deactivation by reduction to S⁴⁺ or reduction of Zr⁴⁺ to Zr³⁺ can not be avoided. At the step of Zr–H formation, Zr⁴⁺ irreversible reduction to Zr³⁺ could be a problem. In the same way, H₂ regenerates the active site by a non-redox reaction with dioxo-site I (see Fig. 5).

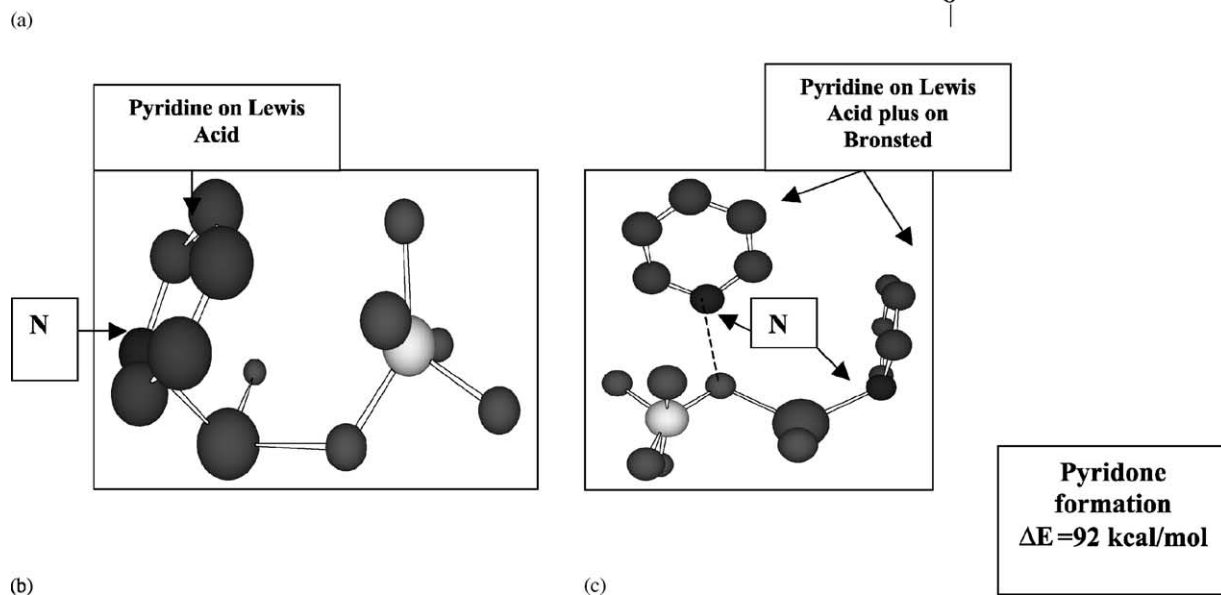
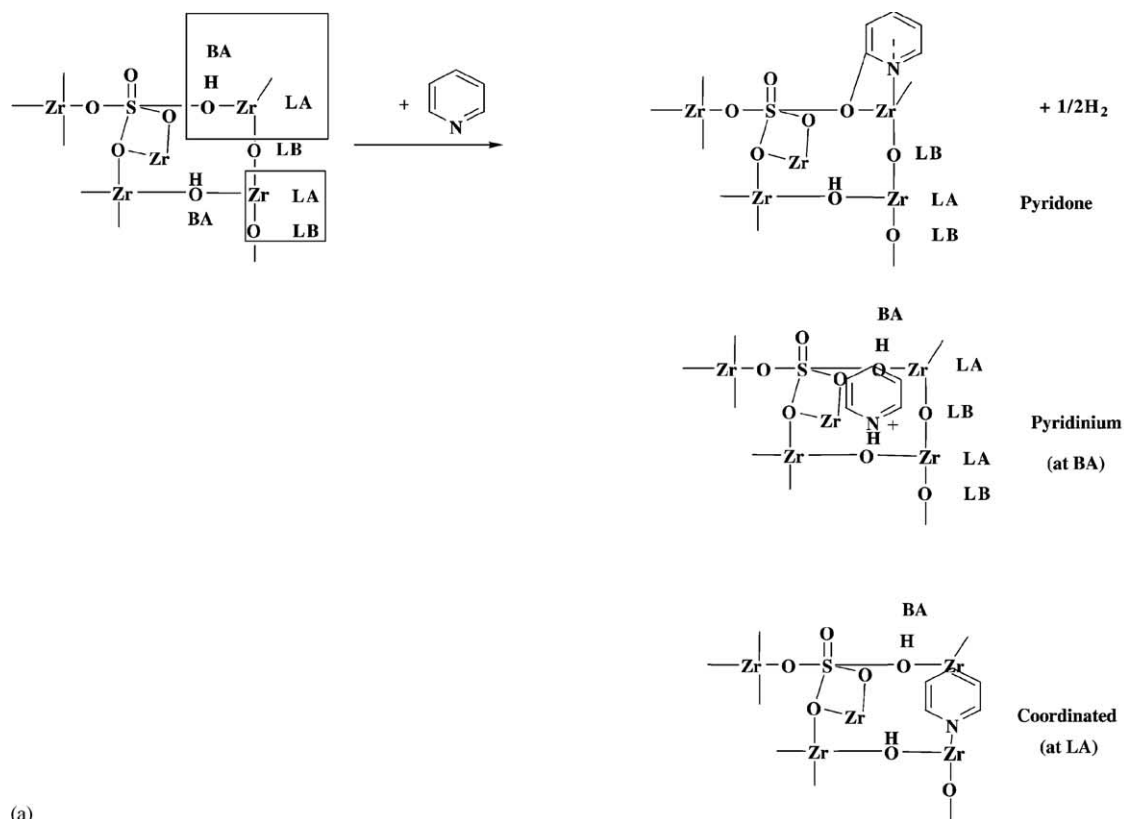


Fig. 9. (a) Scheme of pyridine adsorption on different LA and BA sites; (b) pyridine adsorption on Zr(LA) in site IV vs. steric energy and no H depicted for clarity; (c) pyridine adsorption on Zr(LA) and on Brønsted acid site vs. steric energy and no H depicted for clarity.

Brenner et al. [53] published that no H₂ is found when hydrocarbons are placed in contact with sulfated zirconia. Moreover, Hong et al. [34] found H₂ evolution and these authors could correlate isobutene production with H₂ generation. Knözinger [37] has published that no Raman signals of alkenic or aromatic compounds are observed after contact of SZ with *n*-butane in a flow of H₂ at 200 °C for 2 h. No allylic species are found using H₂–butane streams and 0.2% Pt-SZ. When H₂ is present, hydrocarbon deposits seem to appear only at very low concentration. The monomolecular mechanism has been proposed to be preferred to bimolecular one [48,52]. At low reaction temperatures, not more than 250 °C, addition of hydrogen as carrier gas decreases the conversion comparing it with N₂ as carrier gas. At higher temperatures, it increases the activity. If the pretreatment is done in oxidizing atmosphere-air, the catalyst is more active than under inert atmosphere-N₂. Under reducing atmosphere-H₂, the SZ catalyst is almost inactive [44]. This fact can be easily explained if the Zr³⁺ at surface, no closely related to SOH, is oxidized to Zr⁴⁺ in air. The Zr⁴⁺ can dissociate hydrogen. The surface concentration of hydride is crucial in the *n*-butane isomerization mechanism.

4. Conclusions

The main facts of this proposal are:

- Several redox cycles can be present (for dimeric sites, for Zr⁴⁺/Zr³⁺).
 - Superacidity (if any) would take place in the reaction media. It is related to BA (SOHZr), LA (Zr) and LB (Zr–O–Zr) sites. No superacidity is found in studies with probe molecules before the reaction.
 - Besides the sulfate content and the predominance of the tetragonal crystalline phase, the surface structure is very important in the formation of active sites and intermediaries.
 - Hydrogen and methane evolution can be explained.
 - Brönsted and Lewis acidity can be taken into account.
 - LA–LB pair sites of SZ are proposed to play a very important role.
 - The effects of H₂, CO and butenes on *n*-butane isomerization in SZ can be explained.
- Reported data about FT–IR spectroscopic characterization of SZ before reaction and *n*-butane isomerization support this proposal.

Acknowledgements

The authors want to acknowledge financial support from CONICET (Argentina) and UNS. Besides, we also acknowledge the kind criticism and helpful advices of Prof. Helmut Knözinger (Germany) who helped and encouraged us to improve the article in the way it is now presented.

References

- [1] T. Jin, T. Yamaguchi, K. Tanabe, *J. Phys. Chem.* 90 (1986) 4794.
- [2] T. Yamaguchi, *Appl. Catal.* 1 (1990) 61.
- [3] M. Bensitel, O. Saur, J.C. Lavalley, B.A. Morrow, *Mater. Chem. Phys.* 19 (1988) 147.
- [4] L.M. Kustov, V.B. Kazansky, F. Figueras, D. Tichit, *J. Catal.* 150 (1994) 143.
- [5] F. Haase, J. Sauer, *J. Am. Chem. Soc.* 120 (1998) 13503.
- [6] B. Umansky, J. Engerlhardt, W.K. Hall, *J. Catal.* 127 (1991) 128.
- [7] G. Yaluris, R.B. Larson, J.M. Kobe, M.R. González, K.B. Fogash, J.A. Dumesic, *J. Catal.* 160 (1996) 290.
- [8] M.R. González, J.M. Kobe, K.B. Fogash, J.A. Dumesic, *J. Catal.* 33 (1997) 303.
- [9] H. Armendariz, C. Sanchez Sierra, F. Figueras, B. Coq, C. Mirodatos, F. Lefebvre, D.J. Tichit, *J. Catal.* 171 (1997) 85.
- [10] A. Clearfield, G.P.D. Serrete, A.H. Khazi-Syed, *Catal. Today* 20 (1994) 295.
- [11] B.H. Davis, R.A. Keogh, R. Sirinivasan, *Catal. Today* 20 (1994) 219.
- [12] J.E. Tábora, R.J. Davis, *J. Catal.* 162 (1996) 125.
- [13] F. Babou, B. Bigot, P. Sautel, *J. Phys. Chem.* 97 (1993) 11501.
- [14] C.R. Vera, C.L. Pieck, K. Shimizu, C.A. Querini, J.M. Parera, *J. Catal.* 187 (1999) 39.
- [15] C. Morterra, G. Cerrato, F. Pinna, M. Signoretto, *J. Catal.* 157 (1995) 109.
- [16] F.R. Chen, G. Coudurier, J.F. Joly, J.C. Vedrine, *J. Catal.* 143 (1993) 616.
- [17] E.A. García, E.H. Rueda, A.J. Rouco, *Appl. Catal. A* 210 (2001) 363.
- [18] A. Farcasiu, A. Ghenciu, J. Qi Li, *J. Catal.* 158 (1996) 116.
- [19] K.J. Chao, H.C. Wu, L.J. Leu, *J. Catal.* 157 (1995) 289.
- [20] H. Matsushashi, H. Shibata, H. Nakamura, K. Arata, *Appl. Catal. Part A: Gen.* 187 (1999) 99.
- [21] M. Scheithauer, E. Bosch, U.A. Schubert, H. Knözinger, T.G. Cheung, F.C. Jentoft, B.C. Gates, B. Tesche, *J. Catal.* 177 (1998) 137.

- [22] T. Riemer, D. Spielbauer, M. Hunger, G.A.H. Mekheimer, H. Knözinger, *J. Chem. Soc., Chem. Commun.* 1181 (1994).
- [23] R. White, E. Sikabwe, M.A. Coelho, D. Resasco, *J. Catal.* 157 (1995) 758.
- [24] S. Coman, V. Pârvulescu, P. Grange, V.I. Pârvulescu, *Appl. Catal. Part A: Gen.* 176 (1999) 45.
- [25] D. Spielbauer, G.A.H. Mekheimer, M.I. Zaki, H. Knözinger, *Catal. Lett.* 40 (1996) 71.
- [26] M.J. Frisch, G.W. Trucks, H.B. Schlegel, G.E. Scuseria, M.A. Robb, J.R. Cheeseman, V.G. Zakrzewski, J.A. Montgomery Jr., R.E. Stratmann, J.C. Burant, S. Dapprich, J.M. Millam, A.D. Daniels, K.N. Kudin, M.C. Strain, O. Farkas, J. Tomasi, V. Barone, M. Cossi, R. Cammi, B. Mennucci, C. Pomelli, C. Adamo, J. Clifford, S. Ochterski, G.A. Petersson, P.Y. Ayala, Q. Cui, K. Morokuma, D.K. Malick, A.D. Rabuck, K. Raghavachari, J.B. Foresman, J. Cioslowski, J.V. Ortiz, A.G. Baboul, B.B. Stefanov, G. Liu, A. Liashenko, P. Piskorz, I. Komaromi, R. Gomperts, R.L. Martin, D.J. Fox, T. Keith, M.A. Al-Laham, C.Y. Peng, A. Nanayakkara, M. Challacombe, P.M.W. Gill, B. Johnson, W. Chen, M.W. Wong, J.L. Andres, C. Gonzalez, M. Head-Gordon, E.S. Replogle, J.A. Pople, *Gaussian, Gaussian'98, Revision A.9*, Pittsburgh, PA, 1998.
- [27] T. Kanougi, T. Atoguchi, S. Yao, *J. Mol. Catal. Part A: Chem.* 177 (2002) 289.
- [28] T. Yamaguchi, K. Tanabe, Y.C. Kung, *Mater. Chem. Phys.* 16 (1986) 67.
- [29] V. Adeeva, G.D. Lei, W.M.H. Sachtler, *Appl. Catal. Part A: Gen.* 118 (1994) 1.
- [30] V. Adeeva, J.W. de Haan, J. Jänchen, G. De Lei, V. Scünemann, L.J.M. van de Ven, W.M.H. Sachtler, R.A. van Santen, *J. Catal.* 151 (1995) 364.
- [31] B.H. Davis, R.A. Keogh, S. Alerasool, D.J. Zalwski, D.E. Day, P.K. Doolin, *J. Catal.* 183 (1999) 45.
- [32] R. Keogh, D. Sparks, J. Hu, I. Wender, J.W. Tierney, W. Wang, B.H. Davis, *Energy Fuels* 8 (1994) 755.
- [33] K. Ebitani, K. Noishi, H. Hattori, *J. Catal.* 130 (1991) 257.
- [34] Z. Hong, K.B. Fogash, R.M. Watwe, B. Kim, B.L. Masqueda-Jiménez, M.A. Natal-Santiago, J.M. Hill, J.A. Dumesic, *J. Catal.* 178 (1998) 489.
- [35] B. Li, R. Gonzalez, *Catal. Today* 46 (1998) 55.
- [36] B.C. Gates, J.R. Katzer, G.C.A. Schuit, *Chemistry of Catalytic Processes*, McGraw Hill, New York, 1980.
- [37] H. Knozinger, *Top. Catal.* 6 (1998) 107.
- [38] J.H. Lunsford, H. Sang, S.M. Campbell, C.-H. Liang, R.G. Anthony, *Catal. Lett.* 27 (1994) 305.
- [39] M. Boronat, P. Viruela, A. Corma, *J. Phys. Chem.* 100 (1996) 633.
- [40] T. Yamaguchi, *Catal. Today* 20 (1994) 199.
- [41] M.A. Cohelo, W.E. Alvarez, E.C. Sikabwe, R.L. White, D.E. Resasco, *Catal. Today* 28 (1996) 415.
- [42] Z. Hong, K.B. Fogash, R.M. Watwe, B. Kim, B.L. Masqueda-Jiménez, M.A. Natal-Santiago, J.M. Hill, J.A. Dumesic, *Catal. Today* 51 (1999) 269.
- [43] H. Davis, *Catal. Today* 20 (1994) 219.
- [44] H.K. Mishra, A.K. Dalai, K.M. Parida, S.K. Bej, *Appl. Catal. Part A: Gen.* 217 (2001) 263.
- [45] W. Stichert, F. Schüth, S. Kuba, H. Knözinger, *J. Catal.* 198 (2001) 277.
- [46] C. Morterra, G. Cerrato, *Chem. Phys.* 1 (1999) 2825.
- [47] N. Katada, J. Endo, K. Notsu, N. Yasunobu, N. Naito, M. Niwa, *J. Phys. Chem. B.* 104 (2000) 10321.
- [48] A. Sayari, Y. Yang, X. Song, *J. Catal.* 167 (1997) 346.
- [49] G. Busca, *Catal. Today* 41 (1998) 191.
- [50] <http://webbook.nist.gov/cgi/cbook.cgi?ID=C142085&Units=SI&Mask=281>.
- [51] K. Arata, *Adv. Catal.* 37 (1990) 165.
- [52] J.A. Moreno, G. Poncelet, *Appl. Catal. Part A: Gen.* 210 (2001) 151.
- [53] A. Brenner, T. Schorodt, B. Shi, B.H. Davis, *Catal. Today* 44 (1998) 235.